



Cite this: *Org. Biomol. Chem.*, 2021, **19**, 439

Received 13th October 2020,  
Accepted 3rd December 2020

DOI: 10.1039/d0ob02086a

rs.c.li/obc

## Biocatalytic synthesis of non-vicinal aliphatic diols†

Ana C. Ebrecht,<sup>a</sup> Jasmin C. Aschenbrenner,<sup>id</sup> <sup>a,b</sup> Martha S. Smit <sup>id</sup> <sup>a,b</sup> and Diederik J. Opperman <sup>id</sup> <sup>\*a</sup>

Biocatalysts are receiving increased attention in the field of selective oxyfunctionalization of C–H bonds, with cytochrome P450 monooxygenases (CYP450s), and the related peroxygenases, leading the field. Here we report on the substrate promiscuity of CYP505A30, previously characterized as a fatty acid hydroxylase. In addition to its regioselective oxyfunctionalization of saturated fatty acids ( $\omega$ -1 –  $\omega$ -3 hydroxylation), primary fatty alcohols are also accepted with similar regioselectivities. Moreover, alkanes such as *n*-octane and *n*-decane are also readily accepted, allowing for the production of non-vicinal diols through sequential oxygenation.

## Introduction

Selective oxyfunctionalization of C–H bonds remains a significant challenge in chemical synthesis. This problem is further compounded for compounds without any directing functional groups such as *n*-alkanes. Biocatalysts such as cytochrome P450 monooxygenases (CYP450s),<sup>1</sup> and more recently peroxygenases,<sup>2</sup> have emerged as promising solutions to this problem. With these heme-thiolate biocatalysts, the protein structure provides a scaffold that restricts the binding orientations, thus “selecting” the C–H groups accessible to the heme-cofactor for oxyfunctionalization. A striking example of this is the ability of some CYP450s (including CYP153s and CYP52s) to perform terminal hydroxylation of alkanes and fatty acids.<sup>3</sup>

The CYP450, CYP102A1 (commonly referred to as BM3), has become the workhorse for selective oxyfunctionalization reactions.<sup>4–6</sup> Its prominence is due in part to its ease of production and use and also an available X-ray crystal structure that was solved in the early 1990s,<sup>7,8</sup> allowing catalytic and mechanistic insights.<sup>9,10</sup> CYP102A1 is a self-sufficient CYP450 which does not require auxiliary proteins for activity. For catalytic activity, CYP450s require electrons that are donated, in general, from reduced nicotinamide cofactors (NADH or NADPH). The electrons are sequentially transferred from the reduced cofactors to the CYP450 heme center *via* specific redox partner proteins. Fusion between the CYP450 and these

auxiliary redox partners has the advantage that only a single biocatalyst has to be produced and the reaction mixture only requires the cofactor, molecular oxygen and substrate. In addition, self-sufficient CYP450s are generally considered more efficient and, in some cases, more stable than systems with multiple components.<sup>11</sup>

Members of the CYP102 family of CYP450s are considered fatty acid hydroxylases, catalysing, amongst others, the sub-terminal ( $\omega$ -1 to  $\omega$ -3) hydroxylation of saturated fatty acids.<sup>12</sup> More in-chain hydroxylation activity towards long-chain fatty acids, albeit with low regioselectivity, has been observed for certain members of the CYP102 family.<sup>13</sup> To date, the catalytic scope and corresponding regio-, enantio- and stereoselectivity/specificity of BM3 have been greatly enhanced through directed evolution,<sup>14,15</sup> rational design<sup>16</sup> and the use of decoy molecules.<sup>17–19</sup>

CYP505, a family of self-sufficient fungal CYP450s, has also been classified as fatty acid hydroxylases, based in part on their remarkable sequence similarity to CYP102s, as well as experimental evidence showing sub-terminal ( $\omega$ -1– $\omega$ -3) hydroxylation of C9–C18 fatty acids by CYP505A1 (P450 foxy).<sup>20</sup> However, similar to CYP102s, the true physiological function and *in vivo* substrate for most of the members of this family remains unknown. Recently, the activity of CYP505D6 from *Phanerochaete chrysosporium* was investigated with respect to its 1-dodecanol metabolism. Among the seven CYP505D P450s encoded by *P. chrysosporium*, two (CYP505D4 and D6) showed higher expression profiles when induced with 1-dodecanol compared to dodecanoic acid. Further investigation, however, revealed CYP505D6 to show very little regioselectivity, producing  $\omega$ -1 to  $\omega$ -7 hydroxylated products from 1-dodecanol.<sup>21</sup>

CYP505A30 has previously been described as a fatty acid hydroxylase able to hydroxylate saturated fatty acids (C12–C15)

<sup>a</sup>Department of Biotechnology, University of the Free State, 205 Nelson Mandela Drive, Bloemfontein, 9300, South Africa. E-mail: opperdj@ufs.ac.za

<sup>b</sup>South African DST-NRF Centre of Excellence in Catalysis, c\*change, South Africa

†Electronic supplementary information (ESI) available. See DOI: 10.1039/d0ob02086a

as well as arachidonic acid.<sup>22</sup> The regioselectivity of CYP505A30 mirrors that of BM3, where primarily sub-terminal hydroxylation is observed, albeit in different product ratios. Our research group recently reported on the in-chain ( $\omega$ -7) hydroxylation by the closely related CYP505E3 from *Aspergillus terreus*.<sup>23</sup> Although hydroxylation of saturated fatty acids (C12–C16) was observed, higher product formation (TTNs) was achieved with medium-chain alcohols (C10 and C12) and even decane. Over-hydroxylation was also observed. This sequential reactivity is not uncommon for CYP505s, as CYP505B1 (FUM6) hydroxylates the branched-chain polyketide-amino acid precursor of fumonisin sequentially at the C14 and C15 positions.<sup>24</sup>

All this prompted us to explore the use of CYP505A30 as a fatty alcohol and alkane hydroxylase for the production of aliphatic diols. Whereas the synthesis of vicinal aliphatic diols such as 1,2-diols from alkenes is well established, with the regioselectivity directed by the C=C double bond, the synthesis of non-vicinal aliphatic diols (apart from  $\alpha,\omega$ -diols) are less explored. These aliphatic diols are important building blocks for lubricants and new polymers.<sup>25,26</sup>

## Results and discussion

### Biocatalyst production

Similar to P450 BM3 (CYP102A1), CYP505A30 is a self-sufficient P450, where the N-terminal CYP450 domain is linked to a diflavin reductase domain (similar to the mammalian cytochrome P450 reductase, CPR), requiring NADPH for activity. CYP505A30 and a truncated version consisting of only the heme-domain (CYP505A30HD) were recombinantly expressed in *E. coli*, with both mostly peripherally associated with the membranes. Expression analysis of the CYP505A30 also revealed truncations of the protein that ultimately co-purified with the N-terminally His<sub>6</sub>-tagged enzyme. A C-terminal His<sub>6</sub>-tagged version was therefore created and could be purified to near homogeneity (Fig. S1 and 2†) with an estimated yield of 2 mg L<sup>-1</sup>. The heme-domain was purified as a N-terminally His<sub>6</sub>-tagged protein with yields of up to 9 mg L<sup>-1</sup>.

### Spectral substrate binding

With CYP450s, the binding of the substrate typically induces the displacement of the distal water molecule bound to the catalytic heme-iron, resulting in a change of absorbance in the spectrum of the enzyme. UV-Vis spectra of both the CYP505A30 and the truncated heme-domain, titrated with fatty acids, fatty alcohols and alkanes, were therefore compared. Both the full-length CYP505A30 and the heme-domain bound a range of different substrates tightly, shifting the Soret band from 418 nm to 388 nm, with an isosbestic point around 406 nm (Fig. S3–S8†), characteristic of type I substrate binding.<sup>27,28</sup> The extent of induced high-spin (HS) iron state varied depending on the substrates (Table S1†). The highest absorbance difference observed was for the C12–C16 fatty acids in the full-length enzyme and C14 for the HD, similar to

that reported by Baker and co-workers.<sup>22</sup> The remaining substrates were compared to the HS accumulation observed for tetradecanoic acid (taken as 100%). The fatty alcohols only induced approximately 60% HS in CYP505A30 and even lower (by ca. 10%) in the truncated HD. For the alkanes, the HS accumulation was between 30–60% in the full-length enzyme and 10–20% in the HD.

The titration spectra were also used to estimate the dissociation constants ( $K_D$ ) (Table S1†). Longer chain fatty acids and fatty alcohols exhibited lower  $K_D$  values, particularly for 1-tetradecanol and 1-hexadecanol, with a  $K_D < 1 \mu\text{M}$ , suggesting tighter binding to the enzyme. For alkanes, higher  $K_D$  values were estimated, with little variation between chain lengths. This estimation, however, could be an artifact of the low solubility of alkanes in water (less than 4  $\mu\text{M}$ ),<sup>29</sup> which is lower than the calculated  $K_D$  values. The limitation in the substrate concentration may lead to an overestimation of the affinity for the compound. The same effect applies to 1-hexadecanol since the  $K_D$  value is higher than the solubility of the compound ( $\sim 0.17 \mu\text{M}$ ).<sup>30</sup>

### Kinetic characterization

Steady-state kinetics of CYP505A30 was performed by monitoring the oxidation of NADPH spectrophotometrically at 340 nm. The fatty acids and primary fatty alcohols exhibited Michaelis-Menten behavior (Fig. S9 and S10†). Contrary to CYP505A1 from *Fusarium oxysporum*, which exhibited substrate inhibition for longer chain saturated fatty acids (C14–C16),<sup>31</sup> no substrate inhibition was observed with fatty acids nor with the fatty alcohols tested. With alkanes, however, it was not possible to perform kinetic characterization due to the low solubility of the compounds. Only turnover frequencies ( $k_{\text{obs}}$ ) are reported at substrate concentrations of 10 mM (Table S1†).

Baker *et al.* reported pentadecanoic acid as the preferred substrate of CYP505A30.<sup>22</sup> With the exception of decanoic acid, CYP505A30 exhibited higher  $k_{\text{cat}}$  values for fatty acids compared to the corresponding fatty alcohols (Table S1†). Lower  $K_M$  values for the corresponding fatty alcohols were, however, generally observed. The catalytic efficiency ( $k_{\text{cat}}/K_M$ ) calculated was thus better with the fatty alcohols compared to their fatty acid counterparts/equivalents (Fig. 1). Although 1-dodecanol yielded the best results, the  $k_{\text{cat}}/K_M$  decreased drastically for longer chain fatty alcohols, with 1-tetradecanol and 1-hexadecanol displaying catalytic efficiency 100-fold lower than for tetradecanoic and hexadecanoic acid, respectively. Hydrogen peroxide formation, which partially accounts for reducing equivalents lost to uncoupling, was also measured during the reactions with selected fatty acids, alkanes and fatty alcohols, and found to constitute less than 16% (Table S1†) of the reducing equivalents consumed.

### Biotransformations

Encouraged by the spectral and kinetic characterization, we performed biotransformations to determine the substrate

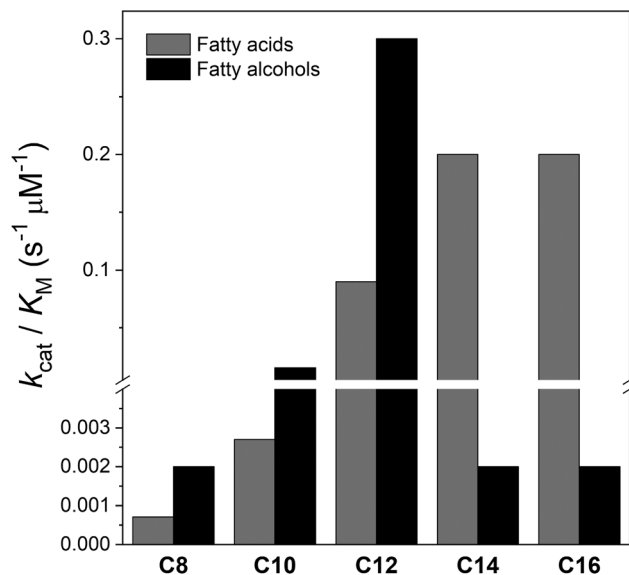


**Fig. 1** Catalytic efficiency of CYP505A30 with different fatty acids and primary fatty alcohols. Reaction conditions: 100 mM potassium phosphate buffer (pH 8), [CYP505A30] = 0.035–1  $\mu\text{M}$ , [NADPH] = 0.3 mM,  $T = 25^\circ\text{C}$ .

scope and regioselectivity of CYP505A30. Reactions (1 mL) were performed with both purified biocatalyst as well as *E. coli* cell free extract (CFE) containing CYP505A30 and allowed to proceed for 0.5–24 h, where after the products were extracted with an equal amount of ethyl acetate, derivatized and analysed by GC-MS. With CFE biotransformations, complete conversion was observed within 2 h for both sets of fatty acids and primary fatty alcohols tested (C8–C12), except for octanoic acid that reached 90% conversion. Product yields from purified enzymes were significantly lower, with even the 24 h reactions not reaching the conversion levels seen with CFE biotransformations after 2 h. This is consistent with our previous results with alkane hydroxylation with CYP450s, where the CFE contributes significantly to the stabilization of the enzyme,<sup>32,33</sup> allowing much higher TTNs. Additionally, the CFE could increase the solubility of these substrate.<sup>34</sup>

Comparable activities were observed between the fatty acids and primary fatty alcohols, with TOF values ranging between 20 and 50  $\text{min}^{-1}$  (Table S2†). The major products observed were  $\omega$ -1 and  $\omega$ -2 hydroxylated fatty acids and fatty alcohols, and  $\omega$ -3 in a lower amount (<8%) (Fig. 2). Baker *et al.* showed hydroxylation of dodecanoic and tetradecanoic acid in the positions  $\omega$ -1 to  $\omega$ -3, with a high ratio of  $\omega$ -1 hydroxylation.<sup>22</sup> Our analysis of the product formation with fatty acids showed the regioselectivity to be dependent on the chain-length. In general, more than 70% hydroxylation in the  $\omega$ -1 position was observed. Upon complete conversion (after 2 h), overhydroxylation of dodecanoic acid occurred. For decanoic acid, overhydroxylated products were only observed at later time points (Fig. S11†). CYP505A30 showed similar regioselectivities with the corresponding primary fatty alcohols, with overoxidation

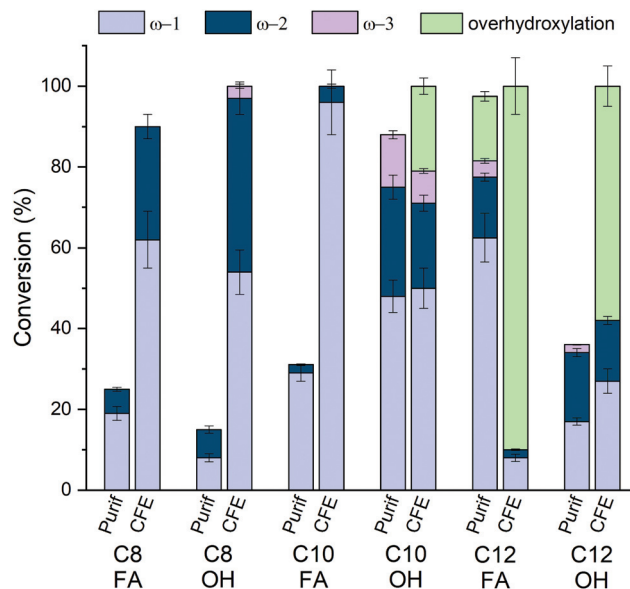


**Fig. 2** Conversion of C8–C12 saturated fatty acids (FA) and primary fatty alcohols (OH) by purified CYP505A30 (Purif) and CYP505A30 within *E. coli* cell free extracts (CFE). Reaction conditions: 200 mM potassium phosphate buffer (pH 8), [CYP505A30] = 4  $\mu\text{M}$ , [*BmGDH*] = 0.2 U  $\text{mL}^{-1}$ , [glucose] = 200 mM, [NADP<sup>+</sup>] = 0.3 mM, [FA or OH] = 10 mM,  $T = 30^\circ\text{C}$ , shaking = 200 rpm,  $t = 24$  h (Purif),  $t = 2$  h (CFE).

(formation of triols) also observed for 1-decanol and 1-dodecanol (Fig. S12†).

In addition to primary fatty alcohols, we also tested the hydroxylation of different secondary fatty alcohols (2-, 3- and 4-octanol, 2-decanol, and 2-dodecanol). The enzyme also accepted all these fatty alcohols as substrates, with near complete conversion within 2 h, except for 3- and 4-octanol (Table 1). The regioselectivities of CYP505A30 was mostly unaltered between the 1-, 2-, and 3-octanol, whereas 4-octanol gave higher amounts of  $\omega$ -1 (C7) or C2 hydroxylated products and no  $\omega$ -3 hydroxylation. The selectivity for  $\omega$ -1 hydroxylation decreased with 2-decanol and 2-dodecanol (Table 1). Reactions again led to triol formation, a behavior seemingly character-

**Table 1** Conversion of fatty alcohols by CYP505A30

	Conv (2 h)	$\omega$ -1	$\omega$ -2	$\omega$ -3	Triols
1-Octanol	>99%	55	42	3	
2-Octanol	>99%	64	33	3	
3-Octanol	83%	53 <sup>a</sup>	24	6	
4-Octanol	71%	53 <sup>a</sup>	18 <sup>b</sup>		
1-Decanol	>99%	44 [19]	27 [7]	6 [2]	23
2-Decanol	>99%	51	46	3	
1-Dodecanol	>99%	27 [18]	15 [11]		58
2-Dodecanol	93%	43 [19]	28 [17]		22

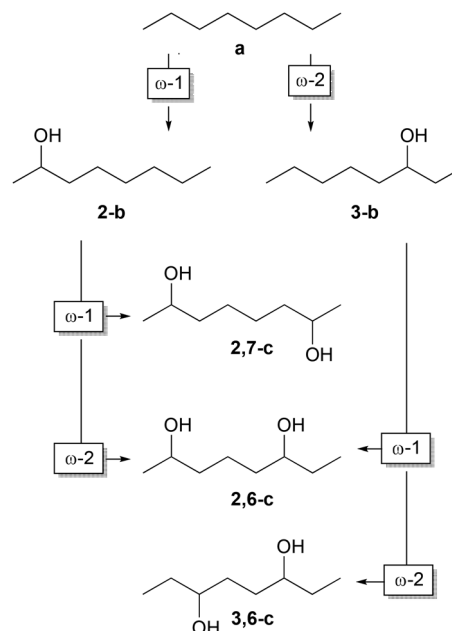
Reaction conditions: 200 mM potassium phosphate buffer (pH 8), 0.8 mL CFE [CYP505A30] = 4  $\mu\text{M}$ , [*BmGDH*] = 0.2 U  $\text{mL}^{-1}$ , [glucose] = 100 mM, [NADP<sup>+</sup>] = 0.3 mM, [alcohol] = 10 mM,  $T = 30^\circ\text{C}$ , shaking = 200 rpm,  $t = 2$  h. Values in brackets  $t = 30$  min. <sup>a</sup>Includes C2 hydroxylation. <sup>b</sup>Includes C3 hydroxylation.

istic of the CYP505 family. *A. terreus* CYP505E3, also exhibited double-hydroxylation of long-chain fatty acids and alcohols, with higher percentages in longer chain substrates.<sup>23</sup>

In addition, the CYP505 FUM6, is also involved in sequential hydroxylation steps of an already functionalized long-chain alkyl substrate as part of its physiological function.<sup>24</sup>

CYP505A30 also catalysed the hydroxylation of *n*-octane and *n*-decane, producing the 2- and 3-alcohols as the major products. Unlike CYP102A1 which only showed mono-hydroxylation events with *n*-octane and *n*-decane,<sup>32,35</sup> the alcohol products served as substrates for CYP505A30 in a second round of hydroxylation to produce various diols.

Higher activity was observed with *n*-octane, with a TOF of *ca.* 74 min<sup>-1</sup> (Table S2†), yielding ~36 mM total products after 24 h (TTN *ca.* 10700). The total product achieved with *n*-octane was remarkable considering the yields reported in the literature. Optimized CYP102A1 mutants reached a maximum of 10 mM products, with a TTN of 4200 at best for the CFE reactions with *n*-octane.<sup>32</sup> Three major diol products were formed, namely 2,7-, 2,6- and 3,6-octanediol (Fig. 3). The symmetrical diols were formed from sequential  $\omega$ -1 or  $\omega$ -2 hydroxylations of *n*-octane, whereas the 2,6-octanediol is a convergent product from either  $\omega$ -1 or  $\omega$ -2 hydroxylation of 3-octanol or 2-octanol respectively (Scheme 1 and S1, Fig. S15†). A similar trend was observed with *n*-decane (Scheme S2, Fig. S15†) despite lower TOF (*ca.* 9 min<sup>-1</sup>) and total products (*ca.* 8 mM, TTN 3100) obtained within the same time period. However, diols consti-



**Scheme 1** Sequential regioselective oxyfunctionalization of *n*-octane in the production of non-vicinal diols.

tuted nearly 60% of the total products, possibly due to the low solubility of *n*-decane and the decanol products formed being the preferred substrate.

Similar product titers were reported with CYP102A1 and its mutants<sup>32</sup> and CYP505E3<sup>23</sup> (*ca.* 5–8 mM), further indicating that substrate solubility could be limiting the reaction. The scalability of the reactions was evaluated by performing a 10 mL reaction with *n*-octane. Despite a reduction in the TTNs to *ca.* 9100, 23.4 mM total product, containing 4 mM diol, was still observed after 24 h, translating to a space time yield (STY) of 3.1 g L<sup>-1</sup> day<sup>-1</sup> in the aqueous phase.

## Conclusions

CYP505A30, characterized initially as a sub-terminal fatty acid hydroxylase, also accepts fatty alcohols and *n*-alkanes as substrates. Similar, or even higher in the case of 1-decanol, catalytic activities and conversions were observed for the shorter chain fatty alcohols compared to the equivalent fatty acids. The regioselectivity of CYP505A30 was unaffected by the nature of the functionalized terminal group. Moreover, this regioselectivity also remained unaffected regardless of the position of the functional group (*i.e.* terminal alcohols *vs.* sub-terminal alcohols). Due to the substrate promiscuity of CYP505A30, *n*-alkanes could be sequentially converted *via* fatty alcohol intermediates to non-vicinal aliphatic diols. We anticipate that similar to CYP102A1,<sup>14,36</sup> the substrate scope and regioselectivity of CYP505A30 is tuneable through directed evolution, which would enable the production of single symmetrical non-vicinal diols. This unique activity opens up new

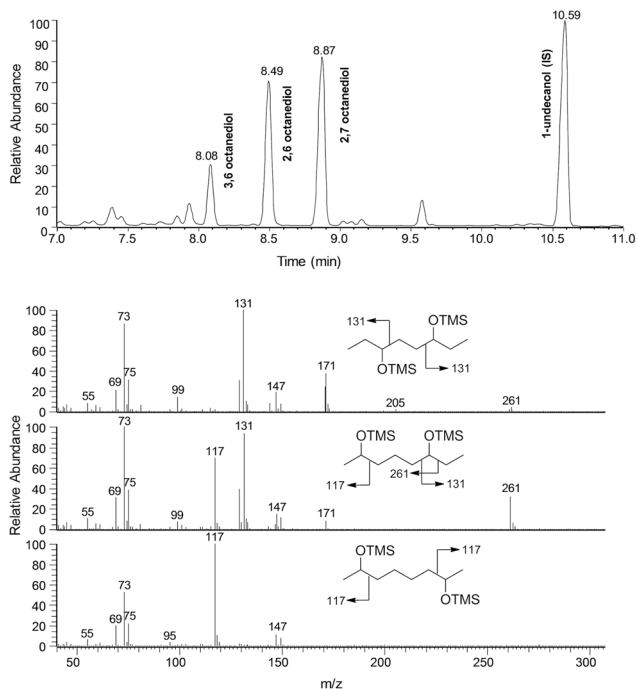


**Fig. 3** GC-MS identification of silylated diols formed during conversion of *n*-octane by CYP505A30. Reaction conditions: 200 mM potassium phosphate buffer (pH 8), [CYP505A30] in CFE (0.8 mL) = 4  $\mu$ M, [BmGDH] = 0.2 U mL<sup>-1</sup>, [glucose] = 200 mM, [NADP<sup>+</sup>] = 0.3 mM, [octane] = 20% (v/v), *T* = 30 °C, shaking = 200 rpm, *t* = 24 h.

routes in polymer chemistry from secondary sub-terminal diols, compared to their  $\alpha,\omega$ -diol counterparts.

## Experimental

### Biocatalyst production and purification

The open reading frame (ORF) coding for CYP505A30 from *Thermothelomyces thermophilus* (*Myceliophthora thermophila*) ATCC 42464 (NCBI CP003004.1) was synthesized and cloned by GenScript into pET28b(+) via *Nde*I and *Hind*III to allow the production of an N-terminal hexahistidine tagged enzyme. The ORF was sub-cloned to pET22b(+) using the same restriction sites. To create a C-terminally hexahistidine tagged version, the stop codon and a part of the plasmid backbone were deleted using inverse PCR with primers CTH-F (5'-CAC CAC CAC CAC TGA GAT C-3') and CTH-R (5'-GTC AAA GAC ATC TGT GGC ATA CCG GTC-3'), as previously described.<sup>37</sup> The CPR domain was similarly removed from the pET28 construct to create a N-terminally hexahistidine tagged variant of only the heme domain (CYP505A30HD) using primers HD-F (5'-TAA AAG CTT GCG GCC GCA CTC GAG CAC-3') and HD-R (5'-GTC TCG AAG AAT GGC CCG CAT GTA GAA GTC-3').

Constructs were transformed into *E. coli* BL21-Gold(DE3) (Stratagene) and selected for on LB-medium supplemented with the appropriate antibiotic (100  $\mu\text{g mL}^{-1}$  ampicillin or 30  $\mu\text{g mL}^{-1}$  kanamycin). Heterologous expression of the CYPs were performed in auto-induction media (ZYP-5052) supplemented with 0.5 mM  $\delta$ -aminolevulinic acid hydrochloride and 50  $\mu\text{M}$   $\text{FeCl}_3 \cdot 6\text{H}_2\text{O}$  (25  $^\circ\text{C}$  for 48 h).

For purification of CYP505A30, cells were harvested by centrifugation (7000g, 10 min, 4  $^\circ\text{C}$ ) and resuspended (0.2 g wet weight  $\text{mL}^{-1}$ ) in buffer A (50 mM potassium phosphate buffer pH 7.4) containing 1% (v/v) Triton X-100. Disruption of the cells was carried out by single passage through a One-Shot Cell disrupter System (Constant Systems Ltd) at 30 kPsi, followed by centrifugation (30 000g, 30 min, 4  $^\circ\text{C}$ ) and ultracentrifugation (100 000g, 90 min, 4  $^\circ\text{C}$ ). The resulting soluble fraction was loaded onto a 5 mL HisTrap FF column (GE Healthcare), previously equilibrated with buffer A. The loaded column was washed with 10 column volumes of buffer A containing 40 mM NaCl and 40 mM imidazole. Protein was eluted using a linear gradient of increasing NaCl and imidazole (40–500 mM). Fractions containing CYP505A30 were pooled, concentrated using ultrafiltration (Amicon Ultra-30 kDa MWCO; Merck), and desalted using PD-10 columns (GE Healthcare) equilibrated with buffer C (50 mM potassium phosphate buffer pH 8.0). The desalted protein was loaded onto a 5 mL HiTrap Q HP column (GE Healthcare), and the protein was eluted using a linear gradient of increasing NaCl (0–500 mM). Finally, size exclusion chromatography (SEC) was performed using Sephacryl S200HR (XK 26 column, GE Healthcare) equilibrated with buffer C containing 100 mM NaCl and 10% (v/v) glycerol. The eluted enzyme was pooled, concentrated, and stored at 4  $^\circ\text{C}$  for up to 5 days. For CYP505A30HD purification, cells were resuspended in buffer B (50 mM potassium phosphate

buffer pH 7.4, 40 mM imidazole, 500 mM NaCl) containing 1% (v/v) Triton X-100. After disruption of the cells and centrifugation, the soluble fraction was loaded onto a HisTrap FF column, and the protein was eluted in a linear gradient of imidazole 40–500 mM. The last step consisted of a SEC using buffer C containing 10% (v/v) glycerol. The enzyme eluted was pooled and concentrated as described above.

*Bacillus megaterium* glucose dehydrogenase (*BmGDH*) was expressed from pET28b(+) and purified as previously described.<sup>38</sup>

Protein concentration was determined by Pierce BCA assay (ThermoFisher Scientific) using bovine serum albumin as a standard. CYP concentrations were determined using CO-difference spectra.

### Steady-state kinetics

Steady-state kinetics were performed by spectrophotometrically monitoring the oxidation of NADPH at 340 nm ( $\epsilon_{340} = 6.22 \text{ mM}^{-1} \text{ cm}^{-1}$ ), in 1 mL reactions containing 100 mM potassium phosphate buffer pH 8, diluted CYP505A30 (0.035–1  $\mu\text{M}$ ). Reactions were initiated by the addition of 0.3 mM NADPH. Substrates were prepared in DMSO. DMSO concentration did not exceed 1% of the total volume in the reaction mixtures. Assays were carried out at 25  $^\circ\text{C}$  in a 1 cm path-length cuvette using a Cary 300 Bio UV/Vis spectrophotometer (Varian). Kinetic constants were determined by non-linear regression to the Michaelis–Menten equation using the Origin software (OriginLab).

Hydrogen peroxide uncoupling was measured as the percentage of NADPH that is used to produce hydrogen peroxide during the reaction. CYP505A30 reactions were performed as described above, containing 0.1 mM NADPH, 0.15  $\mu\text{M}$  CYP505A30 and excess substrate. Reactions were monitored spectrophotometrically until complete consumption of NADPH, where after hydrogen peroxide was quantified using Ampliflu™ Red assay.<sup>39</sup> Ampliflu solution consisted of 100  $\mu\text{M}$  Ampliflu Red, 0.2 U horseradish peroxidase and 2 U superoxide dismutase.

### Substrate binding titrations

Spectral studies of CYP505A30(HD) were performed at 25  $^\circ\text{C}$  in 100 mM potassium phosphate pH 8. Reactions contained 2.5  $\mu\text{M}$  enzyme in a final volume of 1 mL. Stock solutions of substrates were prepared in DMSO, and titrations were performed by the stepwise substrate addition of 0.5–2  $\mu\text{L}$ , with the total volume added never exceeding 1% of the total sample volume. UV-Vis spectra (300–750 nm) were recorded for the substrate-free enzyme, as well as after every titration until no further shifts in the spectra were observed. The difference in absorbance along the spectrum was used for identification of minimum and maximum wavelengths. The difference in absorbance between minimum and maximum were plotted against substrate concentration to determine the dissociation constant ( $K_D$ ). Data were fitted using Michaelis–Menten or Morrison function using Origin software (OriginLab).

## Biotransformations

Biotransformations were performed in 40 mL amber vials, with a reaction mixture consisting of 200 mM potassium phosphate buffer pH 8, 200 mM glucose, 4  $\mu$ M CYP505A30, 0.2 U mL<sup>-1</sup> BmGDH and 0.3 mM NADP<sup>+</sup> in a final volume of 1 mL. Reactions were started with the addition of substrate (10 mM of fatty alcohols or fatty acid or 200  $\mu$ L of alkane) and incubated at 30 °C for 0.5, 2, and 24 hours with shaking (200 rpm). For cell-free extract (CFE) biotransformations cells expressing CYP505A30 were resuspended (0.2 g wet weight cells mL<sup>-1</sup>) in buffer D (200 mM potassium phosphate buffer pH 8, 100 mM glucose) and disrupted as stated above, followed by centrifugation (20 000g, 30 min, 4 °C). CFE (800  $\mu$ L) (4  $\mu$ M) was added to the reaction mixture.

Reactions were stopped and extracted by the addition of 150  $\mu$ L HCl (5 M), followed by 1 mL ethyl acetate containing 2 mM internal standard (1-dodecanol or 1-undecanol). Samples were analysed by GC-FID (Shimadzu GC-2010) and GC-MS (Thermo Scientific TraceGC ultra - Trace DSQ) using the columns and temperature programs described in Table S3.†

For GC-FID analysis, fatty acids samples were methylated by mixing equal volumes of ethyl acetate extracts (100  $\mu$ L) and trimethylsulfonium hydroxide (TMSH) preparation.<sup>40</sup> For GC-MS analysis, samples were silylated. For silylation, 100  $\mu$ L of the ethyl acetate extracts from the biotransformations were dried under N<sub>2</sub> at room temperature. Equal amounts of pyridine and N,O-bis(trimethylsilyl)acetamide containing 2% (w/v) trimethylchlorosilane were added to the dried samples, mixed and incubated at 70 °C for 1 h and analyzed by GC-MS.

## Conflicts of interest

There are no conflicts to declare.

## Acknowledgements

The authors would like to thank Mr Sarel Marais for GC-MS analysis.

## Notes and references

- P. R. Ortiz de Montellano, *Chem. Rev.*, 2010, **110**, 932–948.
- Y. Wang, D. Lan, R. Durrani and F. Hollmann, *Curr. Opin. Chem. Biol.*, 2017, **37**, 1–9.
- L. Hammerer, C. K. Winkler and W. Kroutil, *Catal. Lett.*, 2018, **148**, 787–812.
- S. Eiben, L. Kaysser, S. Maurer, K. Kühnel, V. B. Urlacher and R. D. Schmid, *J. Biotechnol.*, 2006, **124**, 662–669.
- F. H. Arnold and J. C. Lewis, *Chimia*, 2009, **63**, 309–312.
- C. J. C. Whitehouse, S. G. Bell and L. L. Wong, *Chem. Soc. Rev.*, 2012, **41**, 1218–1260.
- K. G. Ravichandran, S. S. Boddupalli, C. A. Hasemann, J. A. Peterson and J. Deisenhofer, *Science*, 1993, **261**, 731–736.
- H. Li and T. L. Poulos, *Nat. Struct. Biol.*, 1997, **4**, 140–146.
- M. A. Noble, C. S. Miles, S. K. Chapman, D. A. Lysek, A. C. Mackay, G. A. Reid, R. P. Hanzlik and A. W. Munro, *Biochem. J.*, 1999, **339**, 371–379.
- L. A. Cowart, J. R. Falck and J. H. Capdevila, *Arch. Biochem. Biophys.*, 2001, **387**, 117–124.
- F. Hannemann, A. Bichet, K. M. Ewen and R. Bernhardt, *Biochim. Biophys. Acta, Gen. Subj.*, 2007, **1770**, 330–344.
- S. S. Boddupalli, R. W. Estabrook and J. A. Peterson, *J. Biol. Chem.*, 1990, **265**, 4233–4239.
- S. D. Munday, N. K. Maddigan, R. J. Young and S. G. Bell, *Biochim. Biophys. Acta, Gen. Subj.*, 2016, **1860**, 1149–1162.
- M. W. Peters, P. Meinhold, A. Glieder and F. H. Arnold, *J. Am. Chem. Soc.*, 2003, **125**, 13442–13450.
- G. D. Roiban and M. T. Reetz, *Chem. Commun.*, 2015, **51**, 2208–2224.
- T. W. B. Ost, C. S. Miles, J. Murdoch, Y. F. Cheung, G. A. Reid, S. K. Chapman and A. W. Munro, *FEBS Lett.*, 2000, **486**, 173–177.
- F. E. Zilly, J. P. Acevedo, W. Augustyniak, A. Deege and M. T. Reetz, *Angew. Chem., Int. Ed.*, 2011, **50**, 2720–2724.
- S. D. Munday, S. Dezvarei and S. G. Bell, *ChemCatChem*, 2016, **8**, 2789–2796.
- S. D. Munday, O. Shoji, Y. Watanabe, L. L. Wong and S. G. Bell, *Chem. Commun.*, 2016, **52**, 1036–1039.
- N. Nakayama, T. Asako and H. Shoun, *J. Biochem.*, 1996, **119**, 435–440.
- K. Sakai, F. Matsuzaki, L. Wise, Y. Sakai, S. Jindou, H. Ichinose, N. Takaya, M. Kato, H. Warilshi and M. Shimizu, *Appl. Environ. Microbiol.*, 2018, **84**, 1–15.
- G. J. Baker, H. M. Girvan, S. Matthews, K. J. McLean, M. Golovanova, T. N. Waltham, S. E. J. Rigby, D. R. Nelson, R. T. Blankley and A. W. Munro, *ACS Omega*, 2017, **2**, 4705–4724.
- M. J. Maseme, A. Pennec, J. van Marwijk, D. J. Opperman and M. S. Smit, *Angew. Chem.*, 2020, **59**, 10359–10362.
- S. Uhlig, M. Busman, D. S. Shane, H. Rønning, F. Rise and R. Proctor, *J. Agric. Food Chem.*, 2012, **60**, 10293–10301.
- S. Igari, S. Mori and Y. Takikawa, *Wear*, 2000, **244**, 180–184.
- S. P. Arnaud, L. Wu, M. A. Wong Chang, J. W. Comerford, T. J. Farmer, M. Schmid, F. Chang, Z. Li and M. Mascal, *Faraday Discuss.*, 2017, **202**, 61–77.
- E. M. Isin and F. P. Guengerich, *Anal. Bioanal. Chem.*, 2008, **392**, 1019–1030.
- K. P. Conner, C. Woods and W. M. Atkins, *Arch. Biochem. Biophys.*, 2011, **507**, 56–65.
- J. A. Riddick, W. B. Bunger and T. K. Sakano, *Organic solvents: physical properties and methods of purification*, Wiley, 4th edn, 1986.
- S. H. Yalkowsky, Y. He and P. Jain, *Handbook of Aqueous Solubility Data: An Extensive Compilation of Aqueous Solubility Data for Organic Compounds*, CRC Press LLC, Boca Raton, FL, 2nd edn, 2003.
- T. Kitazume, A. Tanaka, N. Takaya, A. Nakamura, S. Matsuyama, T. Suzuki and H. Shoun, *Eur. J. Biochem.*, 2002, **269**, 2075–2082.

- 32 A. Pennek, C. L. Jacobs, D. J. Opperman and M. S. Smit, *Adv. Synth. Catal.*, 2015, **357**, 118–130.
- 33 S. Kochius, J. van Marwijk, A. Ebrecht, D. Opperman and M. Smit, *Catalysts*, 2018, **8**, 531.
- 34 A. Mohammadzadeh-K, R. E. Feeney, R. B. Samuels and L. M. Smith, *Biochim. Biophys. Acta*, 1967, **147**, 583–589.
- 35 A. Glieder, E. T. Farinas and F. H. Arnold, *Nat. Biotechnol.*, 2002, **20**, 1135–1139.
- 36 E. Weber, A. Seifert, M. Antonovici, C. Geinitz, J. Pleiss and V. B. Urlacher, *Chem. Commun.*, 2011, **47**, 944–946.
- 37 D. J. Opperman and M. T. Reetz, *ChemBioChem*, 2010, **11**, 2589–2596.
- 38 F. M. Ferroni, C. Tolmie, M. S. Smit and D. J. Opperman, *PLoS One*, 2016, **11**, 1–12.
- 39 L. K. Morlock, D. Böttcher and U. T. Bornscheuer, *Appl. Microbiol. Biotechnol.*, 2018, **102**, 985–994.
- 40 W. Butte, *J. Chromatogr. A*, 1983, **261**, 142–145.